Sonker et al. (2017) Can J Biotech 1(1): 26-37
doi: 10.24870/cjb.2017-000103

Canadian Journal of Biotechnology

ISSN 2560-8304

ORIGINAL RESEARCH PAPER **OPEN ACCESS**

Characterization and *in vitro* antitumor, antibacterial and antifungal activities of green synthesized silver nanoparticles using cell extract of *Nostoc* sp. strain HKAR-2

Arun S. Sonker, Richa, Jainendra Pathak, Rajneesh, Vinod K. Kannaujiya and Rajeshwar P. Sinha*

Laboratory of Photobiology and Molecular Microbiology, Centre of Advanced Study in Botany, Institute of Science, Banaras Hindu University, Varanasi 221005, INDIA

Received: Dec 26, 2016; Revised: Mar 04, 2017; Accepted: Mar 16, 2017

Abstract

In the present study we have made an attempt to develop an eco-friendly, cheap and convenient biological (green) method for the synthesis of silver nanoparticles (AgNPs) using the cell extract of the cyanobacterium *Nostoc* sp. strain HKAR-2. Their anticancerous, antifungal and antibacterial properties were also studied against MCF-7 cells, two fungal strains (*Aspergillus niger* and *Trichoderma harzianum*) and two plant bacterial strains (*Ralstonia solanacearum* and *Xanthomonas campestris*), respectively. The structural, morphological and optical properties of green synthesized AgNPs were determined by UV-VIS spectroscopy, Fourier transform infrared (FTIR) spectroscopy, X-ray diffraction, transmission electron microscopy selected area electron diffraction (TEM-SAED) and scanning electron microscopy (SEM). Spectroscopic analysis showed the peak at 419 nm due to the reduction of $AgNO_3$ into silver ion by cyanobacterial extract indicating surface plasmon resonance (SPR) of the synthesized AgNPs. The XRD pattern of AgNPs showed the characteristic Bragg peaks at (111), (200), (220) and (311) facets of the face centre cubic (fcc) confirming their crystalline nature. FTIR analysis revealed that proteins and amino acids are responsible for the reduction of $AgNO_3$ into Ag^+ as well as for the stability of nanoparticles. Zeta potential confirmed that the charge on the nanoparticles is 1.80 mV which indicates the presence of stable nanoparticles. The results of SEM and TEM confirmed the large agglomerated shape of AgNPs with size ranging between 51-100 nm. The AgNPs showed a dose-dependent cytotoxic activity against human breast cancer MCF-7 cells with IC_{50} of 27.5 µg/ml. They also exhibited excellent antibacterial and antifungal activities.

Keywords: Cyanobacteria, Nanotechnology, Silver nanoparticles, *Nostoc* sp. strain HKAR-2, MCF-7 cells, Anticancerous, Antibacterial, Antifungal properties

Abbreviations: Nanoparticles: NPs, Silver nanoparticles: AgNPs, Double-distilled water: DDW

Introduction

Dependency of human life on nanotechnology dates back to the ancient times. In the 21st century, modern science first time used the term "nano". Metals such as silver (Ag), zinc (Zn) and gold (Au) are being widely used as medicine in the Indian medicinal system. Nanoparticles (NPs) are more biocompatible than the conventional therapeutics, hence, being exploited for drug encapsulation and delivery [1]. In addition, they are also used for catalytic, electrical conducting [2-6] and antimicrobial activity [4, 7-9].

The physical and chemical properties of NPs mainly depend upon the shape, size and surface morphology. Chemical method uses stabilizing agent for the synthesis of NPs to prevent unwanted agglomeration of colloids. Furthermore, the by-products of chemically synthesized metal NPs is very toxic to environment, needs high input of energy and is very expensive. It has been reported by several group of workers that natural sources are also able to reduce metal ion into metal NPs [10, 11], hence, in recent trends biological method using plant extracts for metal NPs synthesis have been suggested as valuable alternative tool as compared to chemical methods [12-14]. In particular, biological methods of AgNPs synthesis using microorganisms [9, 15-19], enzymes [20], fungus [21] and plant tissue or plant extracts [22-24] are preferred recently to the other methods due to its reliability, cost effective synthesis and its cytotoxicity towards bacteria, fungi and tumor cells [25, 26]. AgNPs exhibits a broad spectrum of biocidal and biostatic activity and have plasmonics property in the visible

*Corresponding author: Email: r.p.sinha@gmx.net; rpsinhabhu@gmail.com

region [25]. Silver is not very toxic for humans and other animals as compared to other metals [22, 27]. A number of studies have been done for the synthesis of AgNPs using bacteria, fungi, and algae, but these reports have focused on the use of whole cell masses in synthesis of AgNPs [28-32]. Several recent reports are available in which cell extracts are used for the synthesis of metal NPs [33, 34].

Cyanobacteria are one of the largest and most primitive ancient groups of photoautotrophic prokaryotes on Earth [35]. They are rich source of valuable chemicals, pharmaceuticals, biofuels, several pigments and proteins [33]. The cyanobacterial extract contains multiple types of active biomolecules that are involved in the synthesis and stabilization of the NPs [33, 36]. Recently AgNPs, have been synthesized using the whole cells of non-nitrogen-fixing cyanobacteria such as *Plectonema boryanum* and the marine *Oscillatoria willei* [28, 37]. Some of the cyanobacteria such as *Anabaena* sp., *Calothrix* sp. and *Leptolyngbya* sp. have been reported to synthesize intracellular gold, silver, palladium and platinum NPs [38]. Extraction of NPs formed inside the cell is a very complex process and cost-ineffective. Hence, use of cyanobacterial extract for the synthesis of NPs is being widely practiced these days [9, 18, 19, 39-46].

In the present investigation, we used the cell extract of a hot-spring cyanobacterium *Nostoc* sp. strain HKAR-2 for the synthesis of AgNPs. We also made an attempt to screen the *in vitro* anticancerous, antibacterial and antifungal activity of the green synthesized AgNPs.

Materials and Methods

Preparation of aqueous extract of *Nostoc* sp. strain HKAR-2

The filamentous cyanobacterium *Nostoc* sp. strain HKAR-2, isolated from hot-spring of Rajgir, India [47]. Cultures were grown in BG-11 medium without any nitrogen source (pH 7.0) at 20±2℃ under illumination with daylight fluorescent tubes at a photon flux density of 94 μmol photon m^{-2} s^{-1} at the surface of vessels with a 14/10 light/dark cycle [35]. Growth was analyzed by measuring optical density at 750 nm. Exponentially growing cultures were used for the preparation of cell extract. To prepare the cell extract 200 ml double distilled water (DDW) was added in 5 g dry weight of the cyanobacterium and this mixture was heated up to 70℃ for one hour. After heating, the mixture was allowed to cool at room temperature followed by centrifugation at 10,000 rpm for 30 minutes. After centrifugation the supernatant was collected and stored at 4℃ for further use.

Biosynthesis of AgNPs

For AgNPs synthesis, 5 ml of 1 M $AgNO_3$ was added to 5 ml of cyanobacterial cell-extract. The mixture was then incubated at 25℃ for 120 h. The formation of AgNPs was visualized by observing the color change of the reaction mixture. The flask containing only cell extract served as positive control. Pure $AgNO_3$ solution (1 mM) was taken in a flask separately for negative control. For the synthesis of AgNPs, different parameters such as temperature (20, 40, 60, 80, 100 and 120℃), pH (3, 5 and 7), volume of cyanobacterial extract (1, 2, 3, 4 and 5 ml), $AgNO_3$ concentration (1, 2, 4, 6, 8 and 10 mM), time intervals (0, 12, 24, 48, 72, 96 and 120 h) and different environmental conditions (dark, light, 4℃ and -20℃) were optimized.

Characterization of AgNPs

Ultraviolet-Visible (UV-VIS) spectroscopy

The bioreduction of precursor silver ions was monitored by spectroscopic analysis of the aliquots (3 ml) at desired time intervals. Absorption measurements in the range of 200-1100 nm were carried out using UV-VIS double beam spectrophotometer (2900 Hitachi, Japan) at a resolution of 1 nm.

Fourier transform infrared (FTIR) spectroscopy observations

To check the biomolecular capping on to the surface of AgNPs, the centrifuged and dried sample of AgNPs were subjected to FTIR (Varian 3100 FTIR spectrophotometer) analysis. For FTIR, a small amount of dried biomass was grinded with KBr pellet at room temperature with a resolution of 4 cm^{-1} and the range of 400-4000 cm^{-1}. The FTIR spectra of the extract of *Nostoc* sp. strain HKAR-2 were taken before and after the synthesis of AgNPs.

Size distribution and Zeta potential value

The particle size distribution was done using dynamic light scattering (DLS) measurement and zeta potential value of the AgNPs (suspended in Milli-Q water) were determined by using Beckman coulter Delta Nano C particle size analyzer (Beckman Coulter Inc., USA). The AgNPs were dissolved in physiological saline for zeta potential analysis. Data obtained were analyzed using Zetasizer software.

Scanning electron microscopy (SEM)

The morphology and particle size of the AgNPs were characterized using scanning SEM. Briefly, a thin film of the sample was prepared on a carbon coated copper grid by dropping a very small amount of the sample on the grid, and the extra solution was removed using a blotting paper. The film on the SEM grid were then allowed to dry by putting it under a mercury lamp for 5 min. SEM microphotographs were taken in scanning electron microscope (Quanta -200 FEI, Netherland).

Transmission electron microscopy (TEM)

The size of the green synthesized AgNPs was determined using transmission electron microscopy (TECNAI G2-TWIN-FEI TEM). The sample was prepared by sonicating the biosynthesized AgNPs and after that a drop of aqueous sample was placed on a carbon coated copper grid which was formvar coated. It was then dried under infrared lamp prior to photography. TEM operated at an accelerating voltage of 200 kV.

X-ray diffraction (XRD) analysis

The XRD analysis (PAN analytical X pert PRO Model) was done to determine the dimension of biologically synthesized AgNPs with h, k, l value. The aqueous suspension of AgNPs (45 ml) was centrifuged for 10,000 rpm for 30 min and the pellet was dissolved in 5 ml double distilled water. The suspension was then lyophilized (Christ Alpha 1-2 LD plus) and the diffraction pattern was operated at 40 kV and 30 mA in Cu, K-alpha radiation. The particle size (L) of AgNPs was calculated using following Debye-Scherer's equation: $L= 0.9\lambda/\beta\cos\theta$

where, λ is the wavelength of the X-ray, β is full width and half maximum and θ is the Bragg's angle.

***In vitro* cytotoxicity**

Proliferation/survival of cells after AgNPs exposure was assessed by MTT (3-[4, 5-dimethylthiazol-2-yl] 2, 5-diphenyltetrazolium bromide) assay (purchased from Sigma-Aldrich Company, St. Louis,

MO). Briefly, exponentially growing MCF-7 cell line was seeded in 24 well plates (with a density of 40,000 cells/well/2 ml media) and incubated at 37°C for adherence to the bottom of plate. After 18 h, the media was replaced with 2 ml fresh complete DMEM media. Sterile phosphate buffer saline (PBS) (20 µl) containing different concentration of NPs were added in each well and incubated at 37°C. A plate with AgNP-free phosphate-buffer saline served as control. After 48 h exposure of NPs, cells were washed with sterile PBS for removal of NPs to prevent any interference with MTT reagent. Fresh complete DMEM media (500 µl) containing 0.4 µg of MTT reagent was added to each well and the plate was incubated at 37°C. After 5 h, MTT solution in medium was aspirated off. To achieve solubilization of formed formazan crystals 500 µL of DMSO was added. Microtiter plate was shaken for 10 min and purple color of formazan crystals was calculated by measuring optical density (OD) at 570 nm by using a microplate reader (Spectra Max M2, MTX Lab System). The OD at 630 nm was also observed and measured OD was calculated by subtracting the OD at 630 nm to at 570 nm for background correction. Anticancer activity was expressed with respect to the number of viable cells, i.e., anticancer activity is indirectly proportional to the number of viable cells and this in turn is directly proportional to optical density. Measured OD of cells without any treatment of drug was taken as control. Using the control OD values, the percent inhibition at each concentration of the test agent was calculated by dividing the observed OD value by control OD value and multiplying by 100. The anti-proliferative activity of AgNPs is expressed as the 50% inhibitory concentration (IC_{50}). IC_{50} is defined as the concentration of the test agent that results in a 50% decrease in control level of proliferation.

Antibacterial activity by well diffusion method

The biosynthesized AgNPs were tested for their antibacterial activity by well diffusion method against plant pathogenic bacteria such as *R. solanacearum* and *X. campestris*. The pure cultures of these organisms were routinely sub-cultured on nutrient agar medium at 37°C on rotary shaker at 200 rpm. 100 µl of each strain were swabbed uniformly on the individual plates using sterile glass spreader. Defined wells (3 mm) were made on nutrient agar plates using cork borer. Using micropipette, different concentrations (50, 100 and 150 µl) of AgNPs solution were poured into separate wells on the plates. A number of antibiotics were tested for the sensitivity towards the two bacterial strains. For this study, among all the tested antibiotics, only streptomycin (25 µg/ml) was selected as positive control. DDW was taken as negative control. The plates were then incubated at 37°C for desired time interval (overnight) and the different levels of zone of inhibition were measured.

Antifungal activity by well diffusion method

For screening of antifungal activity of AgNPs, a loopful of two fungal strains such as *A. niger* and *T. harzianum* were placed in the centre of Potato dextrose agar (PDA) plates. Wells of size 3 mm were made on the plates using cork borer and was filled with100 µl of NPs solution. Cumin oil (0.6 µl/ml) was used as positive control [48] and DDW as negative control. The plates were then incubated at 35°C for 18 h and the different levels of zone of inhibition were measured**.**

Statistical analysis

The experiments were repeated thrice for accuracy of the results. All results are presented as mean values of three replicates and statistical analyses were done by one-way analysis of variance.

Results

Formation of AgNPs after the addition of the cell extract of *Nostoc* sp. strain HKAR-2 to $AgNO_3$ solution was tested up to 124 h at 25°C (Fig. 1A-C). The addition of cell extract to $AgNO_3$ solution (1 mM)

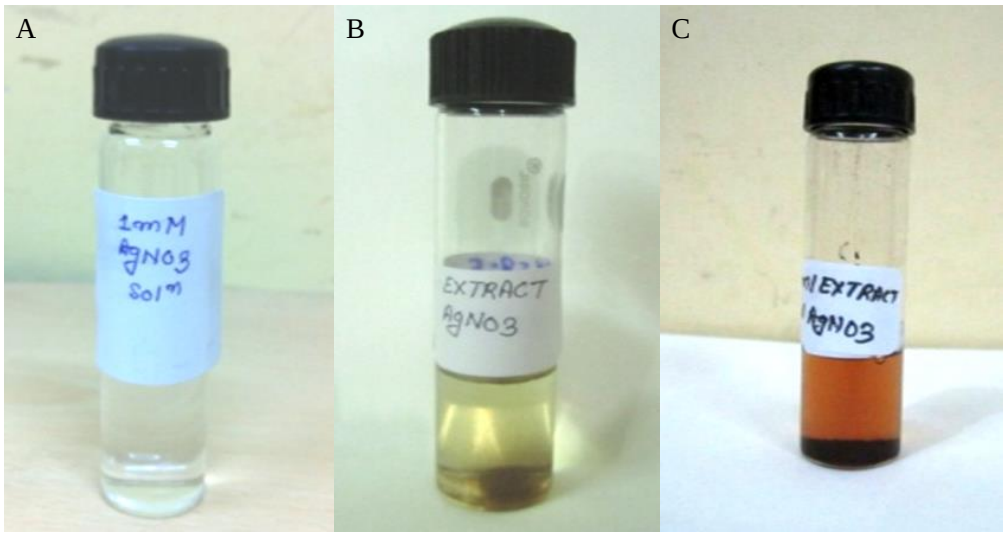

Fig. 1: Change in color of solutions after 124 h of incubation. **(A)** Aqueous $AgNO_3$ solution (colorless), **(B)** *Nostoc* sp. strain HKAR-2 cell extract (light-greenish) and **(C)** reaction mixture containing *Nostoc* sp. strain HKAR-2 cell extract and $AgNO_3$ (1 mM) (brown color). The brown color developed is due to the bioreduction of $AgNO_3$ to Ag^0.

resulted in color change of the reaction mixture from transparent to slightly brownish after 12 h due to the production of AgNPs. The intensity of the color increased with time of incubation, where maximum color change (dark brown) was measured at 124 h (Fig. 1C). On the other hand, the color of $AgNO_3$ solution (colourless; Fig. 1A) and cell extract of *Nostoc* sp. strain HKAR-2 (light green; Fig. 1B) served as a control as they remained unchanged even after 124 h.

An UV-VIS spectrum is one of the most sensitive and easy way to test the synthesis of AgNPs. The absorption peak was recorded at a time interval of 0, 24, 48, 72, 96 and 124 h (Fig. 2). The surface plasmon resonance (SPR) was found to increase at 419 nm at different time interval indicating the maximum synthesis of AgNPs. The reaction mixture gave a broad and strong absorbance peak which is centered at 419 nm and is highly specific for AgNPs. This peak is due to the excitation of SPR of synthesized NPs. With the passage of time, the peak at 419 nm got sharper and narrower due to the rapid production of AgNPs. Among the different parameters, which were used for the effective synthesis of AgNPs, it was observed that the reaction initiated by taking 25 ml of *Nostoc* sp. strain HKAR-2 cell extract with 20 ml of $AgNO_3$ solution (1 mM) at room temperature, neutral pH (7.0), darkness and incubation till 124 h favoured the maximum synthesis of AgNPs. It was noted that the reduction of $AgNO_3$ solution into AgNPs started within 12 h after the addition of $AgNO_3$ solution into cell extract and completed after 124 h. It was observed from the spectra that the SPR at 419 nm showed increased absorbance with increasing incubation time (Fig. 2) indicating the rapid synthesis and stability of biosynthesized AgNPs.

FTIR analysis of the air dried cell extract and AgNPs showed a number of peaks representing different functional group (Fig. 3A-B). The FTIR spectra of dried sample of cell extract of *Nostoc* sp. strain HKAR-2 showed intensive peaks at 3396.25 cm^{-1} (-OH), 2959 cm^{-1} (CH_3), 2923.19 cm^{-1} (C-N) and 1658.5 cm^{-1} (C=O) (Fig. 3A). Whereas the stretching frequencies in biosynthesized AgNPs was observed at 3443.96 cm^{-1} (-OH), 3385.6 cm^{-1} (NH), 2923.83 cm^{-1} (C-N), 2853 cm^{-1} (CH_3) and 1644.73 cm^{-1} (C=O) (Fig. 3B**).** A comparative analysis of the spectra suggested that the cell extract and the AgNPs share common functional groups. These groups indicate that the cyanobacterial extract contain a huge amount of phenolic compound which have the potential to reduce the silver ion into AgNPs. There is a slight change in the frequency between 3396.25 cm^{-1} to 3443.96 cm^{-1} in the cell extract of *Nostoc* sp. strain HKAR-2 during the formation of NPs. The reduction of silver ion into AgNPs might be due to the involvement of –OH group. Band at 2923.19 cm^{-1} (cell extract) and 2923.83 cm^{-1} (synthesized NPs) corresponds to the C-N stretching of the amine. Additionally, waveband of 1644.73 cm^{-1} in biosynthesized nanoparticle could be involved in the adsorption of biomolecule on their surface. Several other peaks in the FTIR spectra indicates the presence of protein which might be responsible of the stability of AgNPs. The nature of the AgNPs formed was detected by using XRD.

The XRD pattern showed four intense peaks ranging from 20^o to 80^o at 2θ. The diffraction peaks at 2θ values of 38.0, 44.0, 64.3, and 77.2^o corresponds to (111), (200), (220) and (311) plane, respectively for silver (Fig. 4). When this spectrum was compared with the available standard, it was found that the biosynthesized AgNPs have crystalline nature.

In addition, three other peaks at 2θ value of 27.52, 32.06 and 45.88^o were also recorded in the XRD data which might be due to the crystallization of the bioorganic phase that are present on the surface of the NPs. The peaks of X-ray diffraction pattern are broad around their bases indicating the nano-size of the biosynthesized AgNPs. The size of the biosynthesized AgNPs were further analyzed using TEM. External morphology of the green synthesized NPs was demonstrated by using SEM. SEM images (Fig. 5) confirmed that the metal

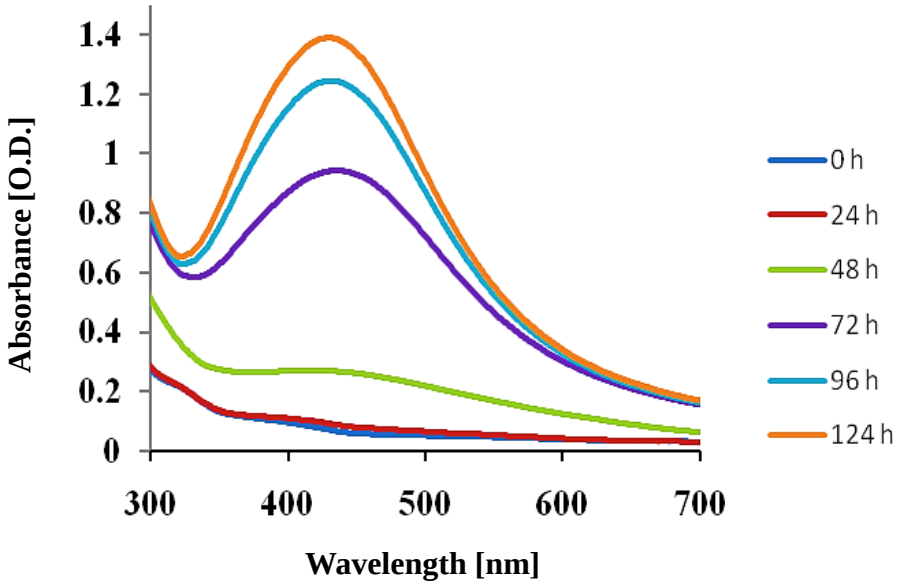

Fig. 2: UV-VIS spectra recorded at different time intervals from aqueous solution of silver nitrate solution with *Nostoc* sp. strain HKAR-2.

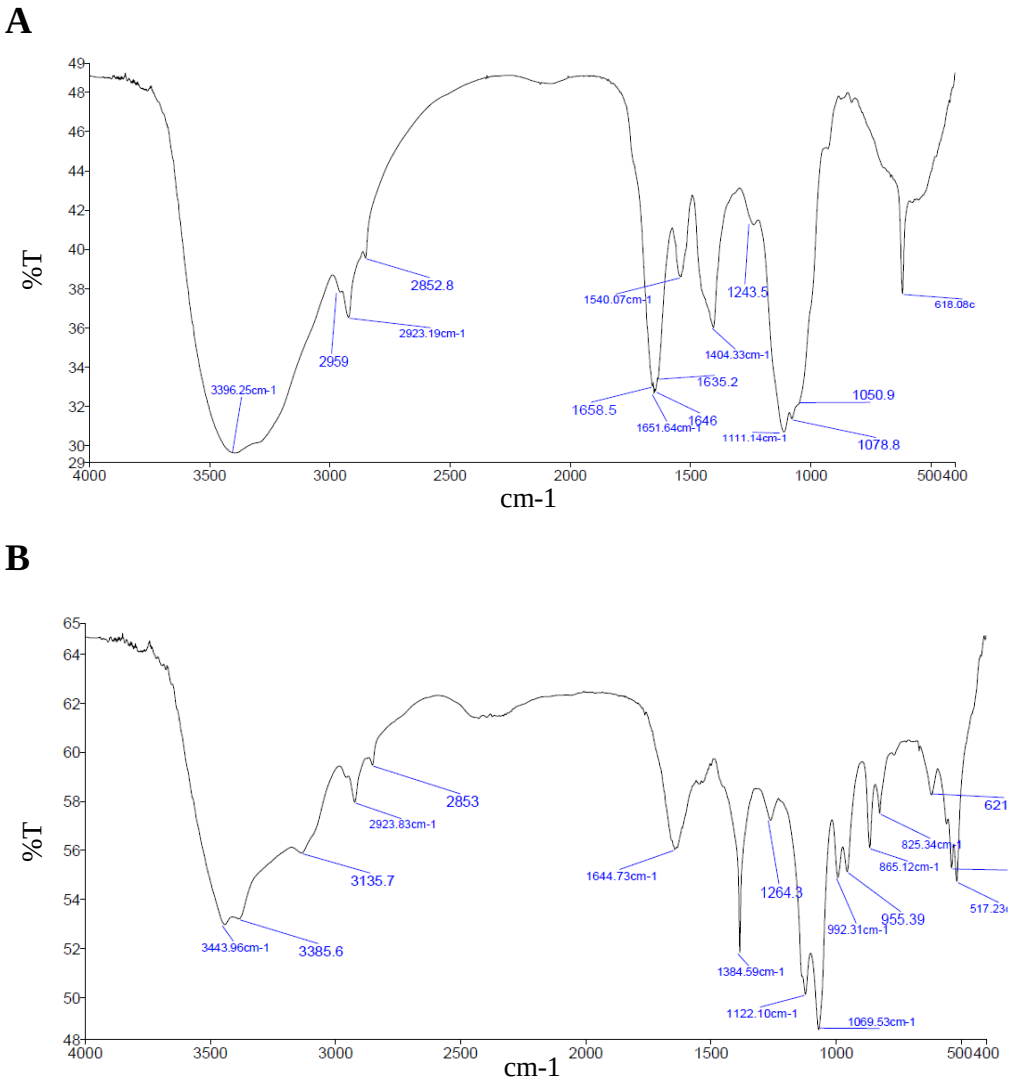

Fig. 3: FTIR spectra of freeze-dried samples of AgNPs. **(A)** *Nostoc* sp. strain HKAR-2 extract without silver nitrate (control) and **(B)** AgNPs synthesized by *Nostoc* sp. strain HKAR-2 extract and $AgNO_3$ (1 mM) solution after 124 h.

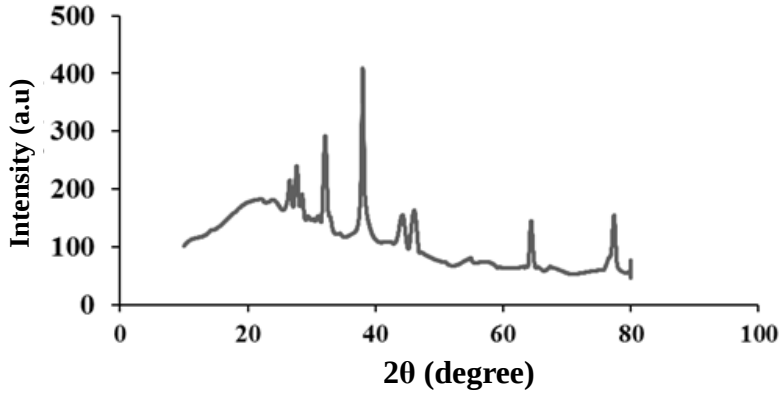

Fig. 4: XRD pattern of AgNPs showing the facets of crystalline silver after bioreduction.

particles are present in nano-size. It is evident from the images that the AgNPs are spherical in shape with an average size of 51-100 µm. The SEM images show small scattered structure (Fig. 5A-C) of biosynthesized AgNPs which then agglomerates into larger size. The magnified view of the NPs which shows the larger images of agglomerated NPs having the size between 51 µm-100µm has been shown in (Fig. 5D-I).

Fig. 6A and 6B shows the TEM images of AgNPs. The size of NPs ranges from 51-100 nm. It is also evident that most of the NPs are spherical and well dispersed in nature. The TEM-SAED pattern showed the clear silver diffraction ring, which is the indication of face cubic centered (FCC) crystalline nature of the AgNPs (Fig. 6C). Some difference in the size of NPs in TEM and DLS is due to the covering of biomolecules on to the NPs.

DLS data show the size distribution of particles with maximum intensity at 255.8 nm (Fig. 7). The Zeta potential showed net charge of 1.80 mV on the AgNPs (Fig. 8). This may be due to the capping of biomolecules onto nanoparticles. The zeta potential mainly depends upon the pH and the electrolytic concentration of the dispersion. Above data supports the stability of NPs in physiological saline pH.

MTT assay was used to analyze the cytotoxic effect of green synthesized NPs on proliferation of MCF-7 cells. The dose dependent cytotoxicity was observed in AgNPs treated MCF-7 cells. The inhibitory concentration (IC_{50}) was determined by considering the concentrations of 50 µg/ml, 20 µg/ml, 10 µg/ml, 5 µg/ml, 2 µg/ml and 0 µg/ml. We dissolved biosynthesized NPs in buffer, which was taken as negative control for MCF-7 cells. However, the cytotoxicity effect of biosynthesized AgNPs against MCF-7 cells did not show significant cytotoxicity at lower concentration and cytotoxicity increased with increasing concentration from 0 µl/ml to 50 µl/ml (Fig. 9).

The antimicrobial activity of AgNPs synthesized by using cyanobacterial extract of *Nostoc* sp. strain HKAR-2 was investigated against two plant pathogenic bacteria i.e. *R. solanacearum* and *X. campestris* by using well diffusion method (data not shown). The diameter of inhibition zones (mm) around each well loaded with AgNPs solution is shown in Table 1. The zone of inhibition formed

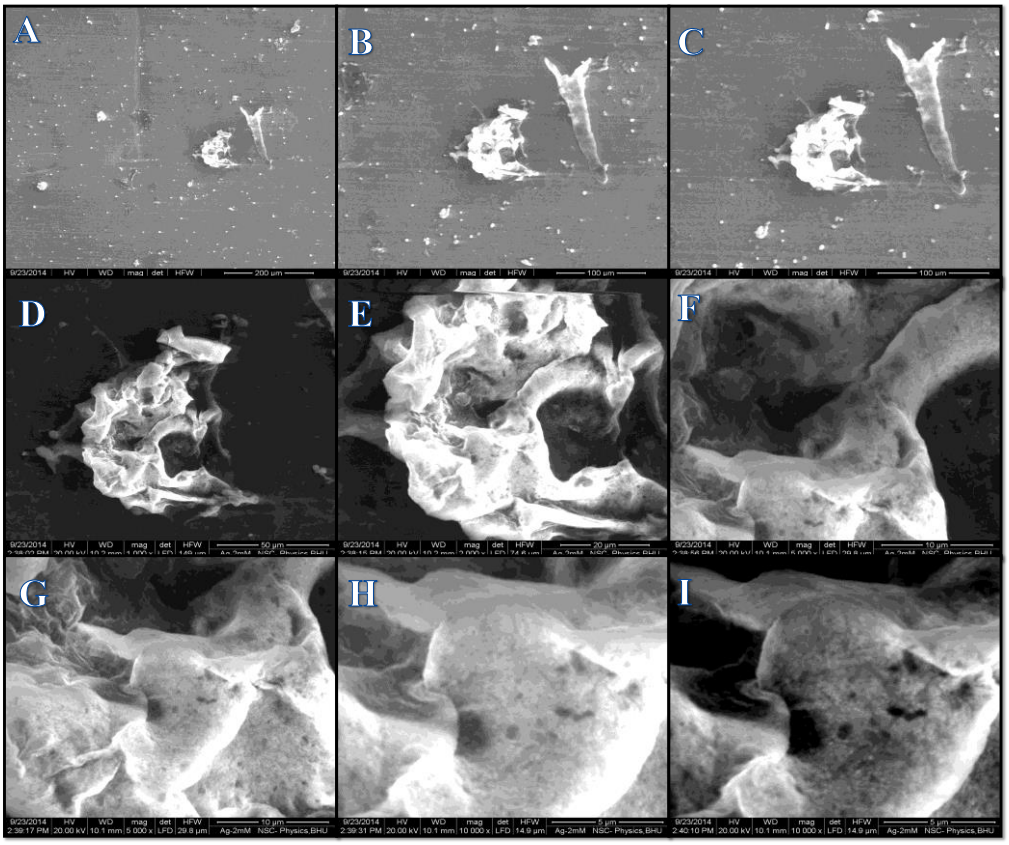

Fig. 5: SEM micrograph images of AgNPs at different magnification synthesized by green method using cyanobacterial extract of *Nostoc* sp. strain HKAR-2 showing the spherical shaped flower like structure. External morphology of the green synthesized nanoparticles is demonstrated by using SEM. The images of SEM from (Fig. 5 A-C) shows small scattered like structure, which are agglomerated into larger size. SEM images from (Fig. 5 D-I) are the magnified view of nanoparticles, which shows the larger images of agglomerated nanoparticles having the size between 51 µm-100 µm.

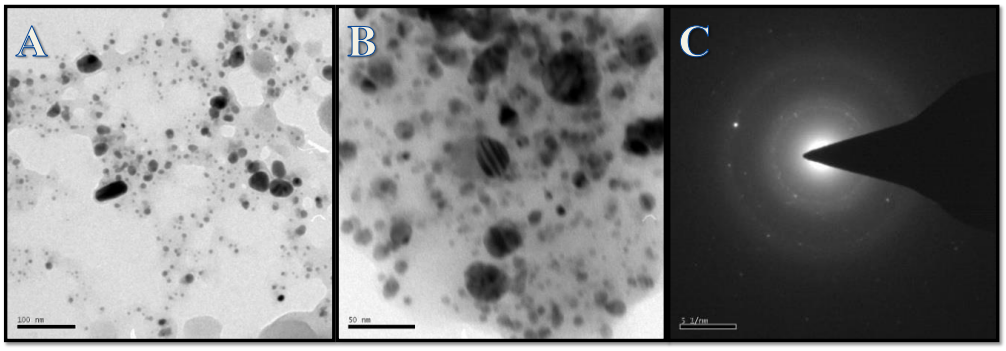

Fig. 6: HRTEM images of AgNPs recorded on carbon coated copper grid synthesized aqueous mixture of *Nostoc* sp. strain HKAR-2 and silver nitrate solution. **(A)** $AgNO_3$ with an average size of 100 nm, **(B)** Spherical AgNPs with an average size of 50 nm synthesized from $AgNO_3$ (1 mM) solution and *Nostoc* sp. strain HKAR-2 extract and **(C)** TEM-SAED ring pattern showing (face-cubic centered) the crystalline nature of AgNPs.

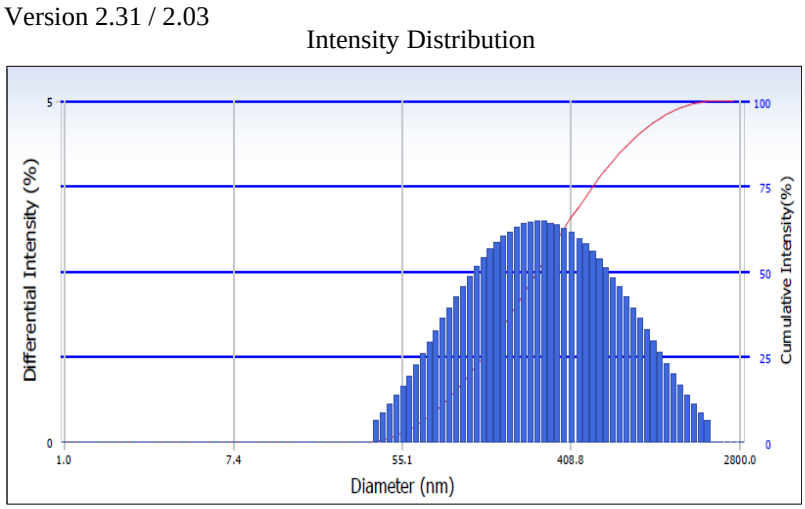

Fig. 7: Size distribution of AgNPs with maximum intensity at 255.8 nm.

by AgNPs against *R. solanacearum* was 15, 25, 25 mm and 18, 23, 23 mm for *X. campestris* at 5, 10 and 15 µg/ml concentration of AgNPs, respectively. The zones of inhibition formed by pure AgNO3 were 11 and 13 mm for *R. solanacearum* and *X. campestris* respectively. DDW was used as a negative control for both the plant bacterial strains and did not show any zone of inhibition around the well of AgNPs whereas antibiotic Streptomycin used as a positive control showed a good zone of inhibition of 35 mm (Table 1).

In the *in vitro* antifungal activity, *Cuminum cyminum* (L.) seed essential oil which is an antifungal [48] agent was used as a positive control for *A. niger* and *T. harzianum* and DDW was used as a negative control for for *A. niger* and *T. harzianum* (data not shown). The diameter of inhibition zones for *A. niger* was found to be 0.3, 0.3 and 0.5 mm and 0.4, 0.4 and 0.5 mm for *T. harzianum* at 5, 10 and 15 µg/ml concentration of biosynthesized AgNPs, respectively (Table 2). Whereas there was no fungal growth in the presence of cumin oil which was taken as a positive control for both the fungal strains, there was a growth of fungi in the presence of DDW which was used as a negative control (Table 2).

Discussion

The synthesis of metal NPs through biological routes has been practiced by several groups of workers [30, 31]. However, only very few reports are available regarding the use of cell extracts of bacteria/cyanobacteria for the synthesis of NPs [32, 33]. The synthesis of AgNPs was initially determined by the color change. Our result clearly shows that the cell extract of the hot-spring cyanobacterium *Nostoc* sp. strain HKAR-2 efficiently reacts with AgNO3 to form AgNPs. The colorr change clearly suggested the possible role of cell extract in reducing the AgNO3 solution into AgNPs. The mechanism how the cyanobacterial cell extract is capable of reducing the AgNO3 solution into AgNPs is not very well

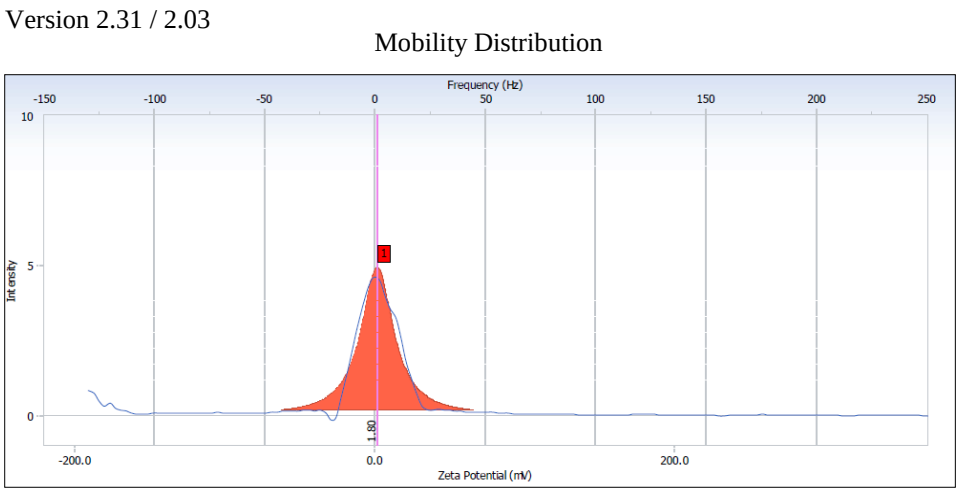

Fig. 8: Biosynthesized AgNPs with a charge of 1.80 mV.

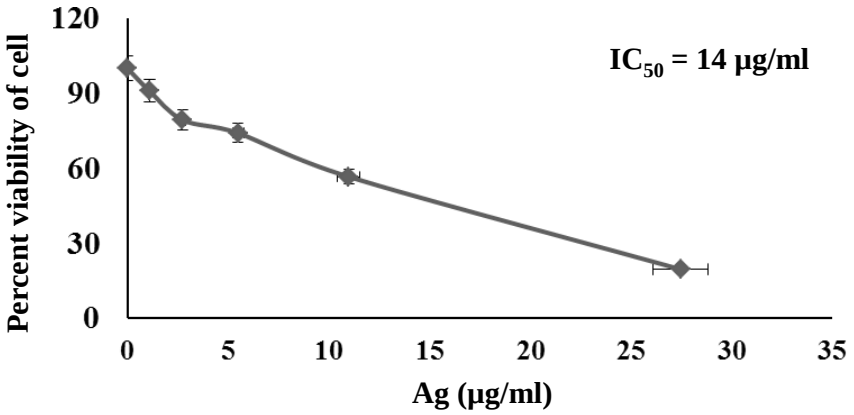

Fig. 9: MTT assay confirming the *in vitro* cytotoxicity effect of AgNPs against the MCF-7 cells. Data was expressed as mean ± SD of three experiments. Percentage of cytotoxicity was expressed relative to untreated controls.

Table 1: Zone of inhibition for AgNPs derived from the cyanobacterium *Nostoc* sp. strain HKAR-2 against plant pathogenic bacterial strains.

Bacteria	Concentration of AgNPs (µg/ml)	Zone of Inhibition (mm)		
		AgNPs	Positive control (Streptomycin)	Negative control (DDW)
R. solanacearum	5	15 ± 4.5	35	0
	10	25 ± 4.0		
	15	25 ± 5.0		
X. campestris	5	18 ± 1.5	35	0
	10	23 ± 4.0		
	15	23 ± 10.0		

*All bacteria were grown under identical conditions and the experiments were performed in triplicate. Plates found with any contamination were immediately discarded. Values represent the mean ± SD.

Table 2: Zone of inhibition for AgNPs derived from the cyanobacterium *Nostoc* sp. strain HKAR-2 against two fungal strains.

Fungal strains	Concentration of AgNPs (µg/ml)	Zone of Inhibition (mm)		
		AgNPs	Positive control (Cumin oil)	Negative control (DDW)
A. niger	5	3 ± 0.03	Full inhibition of growth	Full growth
	10	3 ± 0.06		
	15	5 ± 0.04		
T. harzianum	5	4 ± 0.04	Full inhibition of growth	Full growth
	10	4 ± 0.02		
	15	5 ± 0.10		

*All fungal strains were grown under identical conditions and the experiments were performed in triplicate. Plates found with any contamination were immediately discarded. Values represent the mean ± SD.

known [33, 48], however, it is supposed that the enzyme, protein, amino acids and several other groups might be involved in the reduction of AgNO3 solution into the AgNPs [32, 33, 50]. Some researchers state that a cyanobacterium having an enzyme called nitrate reductase is involved in the reduction of AgNO3 into silver ion [28]. It is also proposed that a number of cyanobacterial photosynthetic pigments and secondary metabolites such as phycobiliproteins, mycosporine-like amino acids (MAAs) and carotenoids are well known photoprotective compounds, present in the cell extract, which might be involved in the synthesis of AgNPs.

UV-VIS spectroscopy is a significant and sensitive technique to authenticate the formation and stability of AgNPs in aqueous solution. Thus, it could be used as the simplest confirmatory tool for metallic NPs synthesis. The appearance of a broad absorption peak at 419 nm specific for AgNPs and the continuous increase in the absorbance with increasing time of incubation clearly indicates gradual increase in production of AgNPs [33, 48]. The data were in accordance with the previously reported spectroscopic data for AgNPs [9], suggesting the potential role of cell extract in the synthesis of metal NPs. FTIR spectra of freeze dried sample of biosynthesized NPs indicate the involvement of different functional group like group of hydroxyl, carboxyl, and carbonyl groups of proteins and amino acids which reduce the AgNO3 solution into the silver ion and stabilized the NPs. Cell extract of *Nostoc* sp. strain HKAR-2 and biosynthesized NPs have the same peak which represents the similar group present in both the sample but major changes in stretching frequencies were noted after the synthesis of AgNPs. Several groups of workers have demonstrated the role of phycobiliproteins in the synthesis and stabilization of metal NPs, probably due to the presence of some aromatic amino acids like tryptophan, phenylalanine and tyrosine which induces the formation of AgNPs [33].

The cell extract of *Nostoc* sp. strain HKAR-2 contains large amount of phycobiliproteins and their role in AgNPs synthesis seems convincing. In FTIR spectra, a few bands assigned to C-N stretching of amino acids belonging to aromatic amino acids group were obtained. In addition to providing stability, capping with biomolecules may provide anchor ability to NPs on bacterial membranes enabling them to attain antibacterial property. The shape, size, solubility and surface charge plays an important role in determining the physical, chemical and biological properties of NPs [30]. In the context of above facts, the size and morphology of the synthesized AgNPs were determined using SEM and TEM, respectively. SEM images revealed the formation of nano-sized spherical AgNPs (51-100 µm). The larger silver particles may be visible due to the aggregation of the smaller ones. TEM showed that the NPs were spherical and well dispersed in nature. It is well established that the production of AgNPs of smaller size is desirable as they show pronounced bactericidal effects possibly due to the availability of large surface area for interaction [49]. Von White et al. [50] have reported that the active biomolecules such as amino acids and small secondary metabolites stabilizes the AgNPs for long duration by avoiding aggregation and growth of NPs.

The crystalline nature of AgNPs having FCC structure was confirmed by TEM-SAED and XRD analysis [51]. Shrivastava et al. [52] have reported that the small size and crystalline structure of NPs responsible for the antimicrobial potentials, are favoured by 111 facets. The zeta potential mainly depends upon the pH and the electrolytic concentration of the dispersion [53]. The zeta potential analysis revealed the surface charge of AgNPs to be -10.950 mV, thereby indicating its prolonged stability even at physiological saline pH. AgNPs are being extensively used in medicine for its therapeutic values. There are only few reports on the cytotoxic effects of biologically synthesized AgNPs against cancer cell lines. Effect of AgNPs on MCF-7 breast cancer cell has already been reported by using *A. squamosa* [54]. To the best of our knowledge, this is the first report regarding the anticancer activity of AgNPs biosynthesized using cyanobacterial cell extract of *Nostoc* sp. HKAR-2 on breast cancer cell lines MCF-7. The dose-dependent cytotoxicity was observed in AgNPs treated MCF-7 cells. The possible cytotoxic mechanism of biosynthesized NPs is not yet clear, but some reports states that the biosynthesized AgNPs disrupts the gene involved in the cell cycle regulation and also induces DNA damage and apoptosis in cancer cells [55].

Owing to strong antibacterial property, silver based compounds are used in medicine from ancient times [32, 56-58]. However, reports on the antibacterial activity of biosynthesized NPs are less [9, 30, 48, 56, 59, 60]. AgNPs have small size with a larger surface area; therefore,

it could be a reason for higher antibacterial activity of AgNPs. Shape, size, solubility and the charge on the biosynthesized NPs played very crucial role in the biological property like inhibiting the growth of bacteria and fungi [30, 61]. Due to the small size and large surface area they have a better surface contact with the bacteria cell surface. This interaction disturbs the cellular function and may cause the defacing of bacterial membrane. The exact mechanism of action of AgNPs as an antibacterial agent is not fully revealed. However, some reports clearly suggests that the AgNPs produces free radicals and these radicals creates pores in the bacterial cell wall changing the membrane permeability, and releases certain vital proteins and lipopolysaccharide molecules [62, 63]. The damages to the bacterial cells may be caused by the interaction of AgNPs with phosphorus and sulfur-containing compounds such as DNA and proteins [32]. NPs have also been reported to inhibit the enzymes of electron transport chain in bacteria, ultimately leading to the cell death [60]. In the present study, we have only confirmed the antibacterial property of AgNPs, but the exact mechanism of their mode of action is still to be deciphered.

Conclusion

In summary, AgNPs have been successfully synthesized biologically by using the cell extract of thermophilic cyanobacterium, *Nostoc* sp. strain HKAR-2 which has a good reducing potential. Various parameters were also optimized for the maximum synthesis of AgNPs. The antitumor property of biosynthesized AgNPs were screened against MCF-7 breast cancer cell line. It was found that AgNPs effectively kill the tumor cells at increasing concentration, suggesting its possible application in the treatment of cancerous cells. Results clearly showed that the biosynthesized AgNPs possessed both antibacterial and antifungal activity. Future research must be focused to understand the mode of action of these nanoparticles as antitumor and antimicrobial agents.

Acknowledgements

AS Sonker is thankful to UGC, New Delhi, India, for the financial support in the form of a fellowship (UGC-JRF-276/S-01). This work was supported in part by DST project (No. SR/WOS-A/LS-140/2011) sanctioned to Richa. J. Pathak and Rajneesh are thankful to CSIR, New Delhi (09/013/0515/2013-EMR-I) and DBT, Govt. of India, (DBT-JRF/13/AL/143/2158), respectively for the financial support in the form of fellowships. The authors acknowledge Department of Physics, BHU and Department of Metallurgical Engineering, IIT, BHU, for the help in characterization of nanoparticles. We are also thankful to Dr. Dinesh Singh, Division of Plant Pathology, IARI, New Delhi, Prof. R. S. Upadhyay and Prof. N. K. Dubey, Department of Botany, BHU, for providing the bacterial, fungal strains and essential oil, respectively. A special note of thanks goes to Manendra Pachauri, Priyanka Rathour and Dhananjay K. Yadav for their help in screening the activities of nanoparticles.

Conflict of Interest

Authors declare no conflict of interest.

References

[1] Wang, X., Yang, L., Chen, Z.G. and Shin, D.M. (2008) Application of nanotechnology in cancer therapy and imaging. *CA Cancer J Clin* 58: 97-110. doi:10.3322/CA.2007.0003

[2] Cuenya B.R. (2010) Synthesis and catalytic properties of metal nanoparticles: Size, shape, support, composition, and oxidation state effects. *Thin Solid Films* 518: 3127-3150. http://dx.doi.org/10.1016/j.tsf.2010.01.018

[3] Kim, J.S., Kuk, E., Yu, K.N., Kim, J.H., Park, S.J., Lee, H.J., Kim, S.H., Park, Y.K., Park, Y.H., Hwang, C.Y., Kim, Y.K., Lee, Y.S., Jeong, D.H. and Cho, M.H. (2007) Antimicrobial effects of silver nanoparticles. *Nanomed Nanotech Biol Med* 3: 95-101. http://dx.doi.org/10.1016/j.nano.2006.12.001

[4] Kumar, V., Yadav, S.C. and Yadav, S.K. (2010) *Syzygium cumini* leaf and seed extract mediated biosynthesis of silver nanoparticles and their characterization. *J Chem Technol Biotechnol* 85: 1301-1309. doi:10.1002/jctb.2427

[5] Rajasekharreddy, P., Rani, P.U. and Sreedhar, B. (2010) Qualitative assessment of silver and gold nanoparticle synthesis in various plants: a photobiological approach. *J Nanopart Res* 12: 1711-1721. doi:10.1007/s11051-010-9894-5

[6] Tripathy, A., Raichur, A.M., Chandrasekaran, N., Prathna, T.C. and Mukherjee, A. (2010) Process variables in biomimetic synthesis of silver nanoparticles by aqueous extract of *Azadirachta indica* (Neem) leaves. *J Nanopart Res* 12: 237-246. doi:10.1007/s11051-009-9602-5

[7] Saravanan, M. and Nanda, A. (2010) Extracellular synthesis of silver bionanoparticles from *Aspergillus clavatus* and its antimicrobial activity against MRSA and MRSE. *Colloids Surf B Biointerfaces* 77: 214-218. http://dx.doi.org/10.1016/j.colsurfb.2010.01.026

[8] Saravanan, M., Vemu, A.K. and Barik, S.K. (2011) Rapid biosynthesis of silver nanoparticles from *Bacillus megaterium* (NCIM 2326) and their antibacterial activity on multi drug resistant clinical pathogens. *Colloids Surf B Biointerfaces* 88: 325-331. http://dx.doi.org/10.1016/j.colsurfb.2011.07.009

[9] Singh, G., Babele, P.K., Shahi, S.K., Sinha, R.P., Tyagi, M.B. and Kumar, A. (2014) Green synthesis of silver nanoparticles using cell extracts of *Anabaena doliolum* and screening of its antibacterial and antitumor activity. *J Microbiol Biotechnol* 24: 1354-1367.

[10] Shankar, S.S., Rai, A., Ahmad, A. and Sastry, M. (2004) Rapid synthesis of Au, Ag, and bimetallic Au core-Ag shell nanoparticles using Neem (*Azadirachta indica*) leaf broth. *J Colloid Interface Sci* 275: 496-502. http://dx.doi.org/10.1016/j.jcis.2004.03.003

[11] Vilchis-Nestor, A.R., Sánchez-Mendieta, V., Camacho-López, M.A., Gómez-Espinosa, R.M., Camacho-López, M.A. and Arenas-Alatorre, J.A. (2008) Solventless synthesis and optical properties of Au and Ag nanoparticles using *Camellia sinensis* extract. *Mater Lett* 62: 3103-3105. http://dx.doi.org/10.1016/j.matlet.2008.01.138

[12] Bhattacharya, D. and Gupta, R.K. (2005) Nanotechnology and potential of microorganisms. *Crit Rev Biotechnol* 25: 199-204. http://dx.doi.org/10.1080/07388550500361994

[13] Mohanpuria, P., Rana, N.K. and Yadav, S.K. (2008) Biosynthesis of nanoparticles: technological concepts and future applications. *J Nanopart Res* 10: 507-517. doi:10.1007/s11051-007-9275-x

[14] Sastry, M., Ahmad, A., Khan, M.I., Kumar, R. (2004)´Microbial nanoparticle production'. In Nanobiotechnology (Niemeyer CM, Mirkin CA, Eds). Wiley-VCH, Weinheim, Germany. 126-135.

[15] Klaus, T., Joerger, R., Olsson, E. and Granqvist, C.G. (1999) Silver-based crystalline nanoparticles, microbially fabricated. *Proc Natl Acad Sci USA* 96: 13611-13614. doi:10.1073/pnas.96.24.13611

[16] Konishi, Y., Ohno, K., Saitoh, N., Nomura, T., Nagamine, S., Hishida, H., Takahashi, Y. and Uruga, T. (2007) Bioreductive deposition of platinum nanoparticles on the bacterium *Shewanella algae*. *J Biotechnol* 128: 648-653. http://dx.doi.org/10.1016/j.jbiotec.2006.11.014

[17] Nair, B. and Pradeep, T. (2002) Coalescence of nanoclusters and formation of submicron crystallites assisted by *Lactobacillus* strains. *Cryst Growth Des* 2: 293-298. doi:10.1021/cg0255164

[18] Sudha, S.S., Rajamanickam, K. and Rengaramanujam, J. (2013) Microalgae mediated synthesis of silver nanoparticles and their antibacterial activity against pathogenic bacteria. *Indian.J Exp Biol* 52: 393-399.

[19] Singh, G., Babele, P.K., Kumar, A., Srivastava, A., Sinha, R.P. and Tyagi, M.B. (2014) Synthesis of ZnO nanoparticles using the cell extract of the cyanobacterium, *Anabaena* strain L31 and its conjugation with UV-B absorbing compound shinorine. *J Photochem Photobiol B* 138: 55-62. http://dx.doi.org/10.1016/j.jphotobiol.2014.04.030

[20] Willner, I., Baron, R. and Willner, B. (2006) Growing metal nanoparticles by enzymes. *Adv Mater* 18: 1109-1120. doi:10.1002/adma.200501865

[21] Vigneshwaran, N., Ashtaputre, N.M., Varadarajan, P.V., Nachane, R.P., Paralikar, K.M. and Balasubramanya, R.H. (2007) Biological synthesis of silver nanoparticles using the fungus *Aspergillus flavus*. *Mater Lett* 61: 1413-1418. http://dx.doi.org/10.1016/j.matlet.2006.07.042

[22] Chandran, S.P., Chaudhary, M., Pasricha, R., Ahmad, A. and Sastry, M. (2006) Synthesis of gold nanotriangles and silver nanoparticles using *Aloe vera* plant extract. *Biotechnol Prog* 22: 577-583. doi:10.1021/bp0501423

[23] Song, J.Y. and Kim, B.S. (2009) Rapid biological synthesis of silver nanoparticles using plant leaf extracts. *Bioprocess Biosyst Eng* 32: 79-84. doi:10.1007/s00449-008-0224-6

[24] Shankar, S.S., Rai, A., Ankamwar, B., Singh, A., Ahmad, A. and Sastry, M. (2004) Biological synthesis of triangular gold nanoprisms. *Nat Mater* 3: 482-488. doi:10.1038/nmat1152

[25] Ghani, A (1998) Medicinal Plants of Bangladesh, Asiatic Society Dhaka, 1st edition, pp: 13.

[26] Kubyshkin, A., Chegodar, D., Katsev, A., Petrosyan, A., Krivorutchenko, Y. and Postnikova, O. (2016) Antimicrobial effects of silver nanoparticles stabilized in solution by sodium alginate. *Biochem Mol Biol J* 2: 13. doi:10.21767/2471-8084.100022

[27] Shah, M.S.A.S., Nag, M., Kalagara, T., Singh, S. and Manorama, S.V. (2008) Silver on PEG-PU-TiO_2 polymer nanocomposite films: An excellent system for antibacterial applications. *Chem Mater* 20: 2455-2460. doi:10.1021/cm7033867

[28] Ali, D.M., Sasikala, M., Gunasekaran, M. and Thajuddin, N. (2011) Biosynthesis and characterization of silver nanoparticles using marine cyanobacterium, *Oscillatoria willei* NTDM01. *Dig J Nanomater Biostruct* 6: 385-390.

[29] Liu, L., Shao, Z., Ang, H.M., Tadé, M.O. and Liu, S. (2014) Are microorganisms indispensable in green microbial nanomaterial synthesis? *RSC Adv* 4: 14564-14568. doi:10.1039/C4RA00555D

[30] Otari, S.V., Patil, R.M., Nadaf, N.H., Ghosh, S.J. and Pawar, S.H. (2014) Green synthesis of silver nanoparticles by microorganism using organic pollutant: its antimicrobial and catalytic application. *Environ Sci Pollut Res Int* 21: 1503-1513. doi:10.1007/s11356-013-1764-0

[31] Prasad, T.N., Kambala, V.S.R. and Naidu, R. (2013) Phyconanotechnology: synthesis of silver nanoparticles using brown marine algae *Cystophora moniliformis* and their characterization. *J Appl Phycol* 25: 177-182. doi:10.1007/s10811-012-9851-z

[32] Sharma, V.K., Yngard, R.A. and Lin, Y. (2009) Silver nanoparticles: green synthesis and their antimicrobial activities. *Adv Colloid Interface Sci* 145: 83-96. http://dx.doi.org/10.1016/j.cis.2008.09.002

[33] MubarakAli, D., Gopinath, V., Rameshbabu, N. and Thajuddin, N (2012) Synthesis and characterization of CdS nanoparticles using C-phycoerythrin from the marine cyanobacteria. *Mater Lett* 74: 8-11. http://dx.doi.org/10.1016/j.matlet.2012.01.026

[34] Shahverdi, A.R., Minaeian, S., Shahverdi, H.R., Jamalifar, H. and Nohi, A.A. (2007) Rapid synthesis of silver nanoparticles using culture supernatants of Enterobacteria: a novel biological approach. *Process Biochem* 42: 919-923. http://dx.doi.org/10.1016/j.procbio.2007.02.005

[35] Rippka, R., Deruelles, J., Waterbury, J.B., Herdman, M. and Stanier, R.Y. (1979) Generic assignments, strain histories and properties of pure cultures of cyanobacteria. *Microbiology* 111: 1-61. doi:10.1099/00221287-111-1-1

[36] Soni, B., Visavadiya, N.P., Dalwadi, N., Madamwar, D., Winder, C. and Khalil, C. (2010) Purified C-phycoerythrin: safety studies in rats and protective role against permanganate-mediated fibroblast-DNA damage. *J Appl Toxicol* 30: 542-550. doi:10.1002/jat.1524

[37] Lengke, M.F., Fleet, M.E. and Southam, G. (2007) Biosynthesis of silver nanoparticles by filamentous cyanobacteria from a silver (I) nitrate complex. *Langmuir* 23: 2694-2699. doi:10.1021/la0613124

[38] Brayner, R., Barberousse, H., Hernadi, M., Djedjat, C., Yepremian, C., Coradin, T., Livage, J., Fievet, F. and Coute, A. (2007) Cyanobacteria as bioreactors for the synthesis of Au, Ag, Pd, and Pt nanoparticles via an enzyme-mediated route. *J Nanosci Nanotechnol* 7: 2696-2708.

[39] Mahdieha, M., Zolanvari A., Azimeea, A.S. and Mahdiehc M. (2012) Green biosynthesis of silver nanoparticles by *Spirulina platensis*. *Sci Iran* 19: 926-929. http://dx.doi.org/10.1016/j.scient.2012.01.010

[40] Ardelean, I.I. (2015) Metallic nanoparticle synthesis by cyanobacteria: fundamentals and applications. In: The Algae World. Springer, Netherlands, pp. 429-448.
[41] Husain, S., Sardar, M. and Fatma, T. (2015) Screening of cyanobacterial extracts for synthesis of silver nanoparticles. *World J Microbiol Biotechnol* 31: 1279-1283. doi:10.1007/s11274-015-1869-3
[42] Lakshmi, P.T.V., Priyanka, D. and Annamalai, A. (2015) Reduction of silver ions by cell free extracts of *Westiellopsis* sp. *Int J Biomater* 539494. http://dx.doi.org/10.1155/2015/539494
[43] Kaliamurthi, S., Selvaraj, G., Çakmak, Z.E. and Çakmak, T. (2016) Production and characterization of spherical thermostable silver nanoparticles from *Spirulina platensis* (Cyanophyceae). *Phycologia* 55: 568-576. http://dx.doi.org/10.2216/15-98.1
[44] Keskin, N.O.S., Kiliç, N.K., Dönmez, G. and Tekinay, T. (2016) Green synthesis of silver nanoparticles using cyanobacteria and evaluation of their photocatalytic and antimicrobial activity. *J Nano Res* 40: 120-127. doi:10.4028/www.scientific.net/JNanoR.40.120
[45] Roychoudhury, P., Ghosh, S. and Pal, R. (2016). Cyanobacteria mediated green synthesis of gold-silver nanoalloy. *J Plant Biochem Biotechnol* 25: 73-78. doi:10.1007/s13562-015-0311-0
[46] Sharma, A., Sharma, S., Sharma, K., Chetri, S.P.K., Vashishtha, A., Singh, P., Kumar, R., Rathi, B. and Agrawal, V. (2016) Algae as crucial organisms in advancing nanotechnology: a systematic review. *J Appl Phycol* 28: 1759-1774. doi:10.1007/s10811-015-0715-1
[47] Rastogi, R.P., Kumari, S., Han, T. and Sinha, R.P. (2012) Molecular characterization of hot spring cyanobacteria and evaluation of their photoprotective compounds. *Can J Microbiol* 58: 719-727. doi:10.1139/w2012-044
[48] Kedia, A., Prakash, B., Mishra, P.K. and Dubey, N.K. (2014) Antifungal and antiaflatoxigenic properties of *Cuminum cyminum* (L.) seed essential oil and its efficacy as a preservative in stored commodities. *Int J Food Microbiol* 168: 1-7. http://dx.doi.org/10.1016/j.ijfoodmicro.2013.10.008
[49] Parashar, U.K., Kumar, V., Bera, T., Saxena, P.S., Nath, G., Srivastava, S.K., Giri, R. and Srivastava, A. (2011) Study of mechanism of enhanced antibacterial activity by green synthesis of silver nanoparticles. *Nanotechnology* 22: 415104-415117. doi:10.1088/0957-4484/22/41/415104
[50] Von White, G., Kerscher, P., Brown, R.M., Morella, J.D., McAllister, W., Dean, D. and Kitchens, C.L. (2012) Green synthesis of robust, biocompatible silver nanoparticles using garlic extract. *J Nanomater* 730746. http://dx.doi.org/10.1155/2012/730746
[51] Choi, H.S., Liu, W., Misra, P., Tanaka, E., Zimmer, J.P., Ipe, B.I., Bawendi, M.G. and Frangioni, J.V. (2007) Renal clearance of quantum dots. *Nat Biotechnol* 25: 1165-1170. doi:10.1038/nbt1340
[52] Shrivastava, S., Bera, T., Roy, A., Singh, G., Ramachandrarao, P. and Dash, D. (2007) Characterization of enhanced antibacterial effects of novel silver nanoparticles. *Nanotechnology* 18: 225103. doi:10.1088/0957-4484/18/22/225103
[53] Muller, R. and Akkar, A. (2004) Drug nanocrystals of poorly soluble drugs. In Encyclopedia of nanoscience and nanotechnology (H.S. Nalwa, Ed). American Scientific Publishers, Stevenson Ranch, 627-638.
[54] Vivek, R., Thangam, R., Muthuchelian, K., Gunasekaran, P., Kaveri, K. and Kannan, S. (2012) Green biosynthesis of silver nanoparticles from *Annona squamosa* leaf extract and its in vitro cytotoxic effect on MCF-7 cells. *Process Biochem* 47: 2405-2410. http://dx.doi.org/10.1016/j.procbio.2012.09.025
[55] Sanpui, P., Chattopadhyay, A. and Ghosh, S.S. (2011) Induction of apoptosis in cancer cells at low silver nanoparticle concentrations using chitosan nanocarrier. *ACS Appl Mater Interfaces* 3: 218-228. doi:10.1021/am100840c
[56] Hsueh, Y.H., Lin, K.S., Ke, W.J., Hsieh, C.T., Chiang, C.L., Tzou, D.Y. and Liu. S.T. (2015) The antimicrobial properties of silver nanoparticles in *Bacillus subtilis* are mediated by released Ag^+ ions. *PLoS ONE* 10: e0144306. doi:10.1371/journal.pone.0144306
[57] Li, P., Li, J., Wu, C., Wu, Q. and Li, J. (2005) Synergistic antibacterial effects of β-lactam antibiotic combined with silver nanoparticles. *Nanotechnology* 16: 1912-1917.
[58] Nowack, B., Krug, H.F. and Height, M. (2011) 120 years of nanosilver history: implications for policy makers. *Environ Sci Technol* 45: 1177-1183. doi:10.1021/es103316q
[59] Duran, N., Marcato, P.D., De Souza, G.I., Alves, O.L. and Esposito, E. (2007) Antibacterial effect of silver nanoparticles produced by fungal process on textile fabrics and their effluent treatment. *J Biomed Nanotechnol* 3: 203-208. https://doi.org/10.1166/jbn.2007.022
[60] Saha, S., Sarkar, J., Chattopadhyay, D., Patra, S., Chakraborty, A. and Acharya, K. (2010) Production of silver nanoparticles by a phytopathogenic fungus *Bipolaris nodulosa* and its antimicrobial activity. *Dig J Nanomater Biostruct* 5: 887-895.
[61] Nel, A., Xia, T., Mädler, L. and Li, N. (2006) Toxic potential of materials at the nanolevel. *Science* 311: 622-627. doi:10.1126/science.1114397
[62] E Lin. Y.S., Vidic, R.D., Stout, J.E., McCartney, C.A. and Yu, V.L. (1998) Inactivation of *Mycobacterium avium* by copper and silver ions. *Water Res* 32: 1997-2000. http://dx.doi.org/10.1016/S0043-1354(97)00460-0
[63] Sondi, I. and Salopek-Sondi, B. (2004) Silver nanoparticles as antimicrobial agent: a case study on *E. coli* as a model for Gram-negative bacteria. *J Colloid Interface Sci* 275: 177-182. http://dx.doi.org/10.1016/j.jcis.2004.02.012